On the End-to-End Delay in a One-Way VANET

Article *in* IEEE Transactions on Vehicular Technology · May 2019

DOI: 10.1109/TVT.2019.2916936

4 authors, including:

Hafez Seliem
Memorial University of Newfoundland
15 PUBLICATIONS **101** CITATIONS
SEE PROFILE

Reza Shahidi
Memorial University of Newfoundland
48 PUBLICATIONS **223** CITATIONS
SEE PROFILE

Mohamed Hossam Ahmed
University of Ottawa
184 PUBLICATIONS **4,421** CITATIONS
SEE PROFILE

On the End-to-End Delay in a One-Way VANET

Hafez Seliem, Reza Shahidi, Mohamed H. Ahmed, Mohamed S. Shehata
Faculty of Engineering and Applied Science, Memorial University of Newfoundland, St. John's, NL, Canada
Email: {hms117, d97rs, mhahmed, mshehata}@mun.ca

***Abstract*—There has been much increased interest in the academic and industrial research communities on vehicular ad-hoc networks (VANETs). In this paper, we present an analytical model to study the end-to-end delay in a one-way VANET. This paper proposes an analytical formula for the end-to-end delay probability distribution. Using the derived probability distribution, the probability that the end-to-end delay is lower than a given threshold may be calculated. In addition, one can straightforwardly study the impact of parameters such as wireless communication range, vehicular densities, distance between source the destination, and minimum and maximum vehicle speeds on the end-to-end delay. This can help to better understand data dissemination in VANETs. Moreover, closed forms for lower and upper bounds on the end-to-end delay probability distribution are obtained. Extensive simulation results demonstrate the accuracy of our analysis.**

I. Introduction

Vehicular ad-hoc networks (VANETs) have attracted the attention of many in the academic and industrial communities. In addition, most new vehicles are now equipped with global positioning systems (GPSs) [1] as well as wireless communication and computational devices. In addition, Dedicated Short Range Communications (DSRC) [2] has been designed to enable ad-hoc wireless communication among vehicles, or vehicles and other infrastructure units such as road-side units (RSUs). Besides safety applications for drivers and passengers, VANETs can provide comfort applications (e.g., weather information, instant messaging, and mobile e-commerce) [3].

VANET connectivity often changes, especially when the vehicular density is low. Therefore, regular ad-hoc routing protocols are not feasible since the routing path is often disconnected on account of the intermittent nature of the network links. Consequently, the packet loss probability increases. To overcome this problem, many proposed VANET routing protocols use a carry-and-forward strategy. In such a strategy, when the vehicles are connected as a cluster, packets can be relayed quickly within the cluster using wireless communications; when VANETs have disconnected clusters, a vehicle can act as a carrier for the packet, and then when the vehicle gets within the wireless communication range of another vehicle, the forwarding process for the packets can be started.

It is important to investigate and determine the probability and statistical characteristics of the end-to-end packet delivery delay in ad-hoc communication networks such as VANETs, (see [4]-[15]). However, it is difficult to characterize the end-to-end delay in VANETs, especially when considering VANETs without infrastructure. Also, the analysis becomes more challenging when considering a random speed distribution for the vehicles as considered in the proposed analysis.

The main contributions of this paper are as follows:

1) It proposes an analytical framework for the CDF of the end-to-end delay in a VANET conditioned on the distance between the source and the destination.
2) It derives a closed-form expression for the lower bound of the end-to-end delay probability density distribution.
3) It proposes a closed-form expression for the upper bound of the end-to-end delay probability density distribution.
4) It presents a comparison between results from the proposed analytical study and simulation results to validate our analysis.

The rest of this article is organized as follows. Section II provides the related work. Section III presents the system model for the proposed analysis. Section IV proposes a formula to determine the CDF of the end-to-end delay in a VANET. Section V derives a closed-form expression for the lower bound of the end-to-end delay probability density distribution. Furthermore, Section VI proposes a closed-form expression for the lower bound of the end-to-end delay probability density distribution. Next, Section VII presents a comparison between the simulation and analytical results as well as a comparison between our result and those from previous works. Subsequently, Section VIII investigates the VANET parameters (vehicle wireless communication range r, different speed range with the same average speed, different average speeds, and distance) and their effect on the end-to-end delay. Then, the conclusions and future work are given in Section IX, and finally the Appendix is added to present derivation details.

II. Related Work

Many papers have analyzed the delay performance in VANETs. However, most of the proposed analytical models focus mainly on connectivity analysis (propagation speed and time) and the expected value of the end-to-end packet delivery delay, not on the probability distribution of the end-to-end packet delivery delay (see [4]-[10]).

Ref. [4] derived the mean packet propagation delay while considering vehicular velocity distributions and inter-vehicle spacing. In addition, based on a discrete-time Markov model, Ref. [5] derived a closed-form expression for a single re-healing delay and then calculated the expected value of the packet propagation speed. Both [4] and [5] used the same system model except that [5] used a Gaussian distribution and [4] used the uniform distribution for each vehicle's speed. An analytical model for multiple traffic streams was proposed in [6]. Moreover, an expression for the mean re-healing delay for packet transmission between two disconnected vehicles on a two-way highway was found in [7]. In addition, the authors

in [8] derived the expected value of the end-to-end delivery delay from a vehicle to Internet access points. Moreover, an analytical expression was proposed for the expected value of the delay of a path in two-way VANETs. Furthermore, using queuing theory, an analysis of the total delay from source to destination in two-way VANETs with traffic lights was proposed in [9]. Moreover, an analytical expression for the expected delay for a source-to-destination path is proposed in [10], in the case of a one-way VANET with the vehicles' speeds following a truncated normal distribution. The authors of [10] extended their work to the case of a bidirectional VANET in [11].

Analytical studies on the delays in VANETs have been proposed which follow the constant-speed model (the vehicles' speeds in the model are equal to the same constant). For instance, the authors in [12] proposed a probabilistic vehicle-to-RSU packet delivery delay model. Their model depends on the effective capacity concept and effective bandwidth theory. In addition, the authors in [13] derived a closed-form expression for the cumulative distribution function (CDF) of the vehicle-to-RSU packet delay in bidirectional highway VANETs conditioned on the inter-RSU distance. Ref. [14] derived upper and lower-bounds on the end-to-end delay in epidemic routing. However, the authors in [9]-[11] considered a constant speed for the vehicles and a fixed location for the destination (RSU or intersection).

In addition, research has been performed on the re-healing delay in VANETs (time taken to forward a packet from a cluster head to the next cluster's tail). For instance, in [15], a closed-form expression was proposed for the unconditional probability distribution of a single re-healing delay in a one-way highway VANET, and this closed-form expression provides a basis for our work. On the other hand, Ref [16] derived an analytical expression for the end-to-end delay and closed-form expressions for the CDFs of the distances travelled by the head and tail of a cluster. In this paper, we propose a more accurate probability distribution than that provided in [16], based on the closed form of the re-healing delay proposed in [15]. On the other hand, Ref. [16] is based on an uncorrected analytical form of the unconditional re-healing delay, the correction for which is proposed in [15]. Moreover, this paper proposes a lower-complexity analytical model for the end-to-end delay probability distribution based on the probability mass function (PMF) of the number of gaps between source and destination, and the closed-form expression for the probability density distribution (PDF) of a single re-healing delay (the model in this paper has one summation over iterated convolutions over the closed-form expression for the PDF of the re-healing delay, while the previous work must perform a summation over repeated convolutions of a numerically-calculated double integral). Furthermore, in this paper, we propose a closed-form expression for the lower and upper bounds of the end-to-end delay probability distribution, allowing one to rapidly find bounds on the worst-case and best-case of the end-to-end delay for a VANET. In addition, the work in [16] was extended to bidirectional highway VANETs in [17]. An analytical expression for the end-to-end delay probability distribution was proposed considering the same system model as in [16], except taking into consideration two directions of motion for the vehicles.

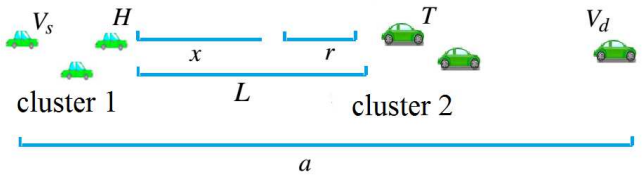

Fig. 1. A VANET with two clusters.

Ref. [18] derived closed-form expressions for the PMF of the number of clusters in a VANET conditioned on distance, and we use this result in our work. In addition, that work calculated the expected delivery delay over this number of gaps.

All this previous work shows that great effort has been exerted towards analyzing the end-to-end packet delay analysis in VANETs and its probability characteristics. However, [4]-[11] considered a constant-speed model or only calculated the expected value of the end-to-end delay in VANETs. On the other hand, in this paper, we propose an analytical framework for calculation of the CDF of the end-to-end propagation delay conditioned on the initial distance from a source to a destination, while the source and the destination are moving with a uniformly-random distributed speed. Deriving the CDF of the end-to-end delay enables one to determine the end-to-end delay statistics (e.g., PDF, moments, and characteristic function). In addition, derivation of the CDF allows one to obtain the probability that the end-to-end packet delivery delay is lower than a given threshold. This allows a service provider, e.g., a service provider of the intelligent transportation system (ITS) to characterize the end-to-end propagation delay based on VANET parameters such as vehicular density, minimum and maximum speeds, wireless communication range, and initial distance between source and destination. Moreover, closed-form expressions for lower and upper bounds on the end-to-end delay probability density distribution are derived, allowing a service provider to rapidly find a bound on the worst-case end-to-end delay for a VANET. The lower bound is important as it represents the worst case for the end-to-end packet delay.

III. System Model

Usually, VANETs are made up of a group of disconnected VANET clusters [15], [16], where a cluster is a maximal set of vehicles in which there is at least one multihop path for every pair of vehicles in the cluster. As shown in Fig. 1, H is the cluster head of cluster 1 and T is the cluster tail of cluster 2.

In the proposed analysis, the vehicles' speeds are assumed to be uniformly distributed between the values of $v_{\min}$ and $v_{\max}$ [4], [16]. In addition, the inter-vehicle distance is assumed to follow an exponential distribution with parameter λ_s, and vehicle arrivals are assumed to follow a Poisson distribution with a rate parameter equal to the vehicular density

$$F_{T_r}(t) = 2\lambda e^{-\left(k_2+k_1+\lambda t+\frac{2\lambda(r-v_{\min}t)}{v_{\max}+v_{\min}}\right)}\left(v_{\min}e^{k_2} - v_{\max}e^{k_2} + v_{\max}e^{k_1+\lambda t} - v_{\min}e^{k_1+\lambda t} - \lambda t v_{\max}e^{k_1+\lambda t} + \lambda t v_{\min}e^{k_1+\lambda t}\right.$$
$$\left. + \frac{2\lambda t e^{k_1+\lambda t}(v_{\max}^2 + v_{\min}^2 - 2v_{\max}v_{\min})}{v_{\max}+v_{\min}}\right) / \left(t(v_{\max}+v_{\min})\left(\lambda + \frac{2(\lambda v_{\min} - \lambda v_{\max})}{v_{\max}+v_{\min}}\right)^2\right) - e^{-\left(k_2-k_1+\frac{2\lambda r}{v_{\max}+v_{\min}}\right)} + 1 \quad (1)$$

where

$k_1 = 2\lambda v_{\min}t/(v_{\max}+v_{\min}),\ \ k_2 = 2\lambda v_{\max}t/(v_{\max}+v_{\min}).$

Table I
LIST OF NOTATION

L	Inter-cluster distance
a	Distance between source and destination
r	Wireless range of a vehicle
T_r	R.V. for the re-healing delay
$F_{T_r}(t)$	CDF of T_r
$f_{T_r}(t)$	PDF of T_r
$X(t)$	R.V. for distance moved by the head of a cluster over the time interval [0,t]
$f_{X(t)}(x)$	PDF of $X(t)$
T_d	End-to-end propagation delay
$X'(t)$	R.V. for distance moved by the tail of a cluster over the time interval [0,t]
$F_{X'(t)}(x)$	CDF of $X'(t)$
λ	Vehicular density (vehicles/second)
λ_s	Inter-vehicle mean distance
$v_{\min}$	Minimum value for the vehicles' speed
$v_{\max}$	Maximum value for the vehicles' speed
Δv	Difference between $v_{\max}$ and $v_{\min}$
$u(\cdot)$	Heaviside step function
$*^i$	Convolution iterated i times
$\mathscr{L}_x[\cdot]$	Laplace transform with respect to x
$\star$	Cross-correlation between two functions
s^*	Complex conjugate of s
$\mathscr{L}_s^{-1}[\cdot]$	Inverse Laplace transform with respect to s
$P_X(x)$	PMF of X
$F_x(\omega)$	Fourier transform with respect to x
$\mathscr{F}_\omega^{-1}$	Inverse Fourier transform relative to ω

λ (vehicles/sec) [3]-[13]. Furthermore, vehicle positions and velocities are assumed to be mutually independent [3]-[8].

In addition, we consider that every pair of vehicles can communicate directly if the Euclidean distance between them is shorter than the vehicle wireless communication range r. Moreover, as in [3]-[8], the delay in receiving and processing the packet before it is available for relaying and forwarding is neglected. This assumption is reasonable as long as IEEE 802.11p supports 3 Mbps for the data rate [19]. Consequently, the delays in transmission and processing of the packet are on the order of tens of milliseconds [16], [20]. Therefore, it can be neglected compared to the delay time in the carry-and-forward strategy. Accordingly, we assume that the end-to-end delay is the sum of the re-healing delays between disconnected vehicle clusters.

Furthermore, we consider a highway with vehicles moving in one direction as shown in Fig. 1. In addition, the list of notations used in the proposed analysis is shown in Table I. Moreover, we assume the vehicle wireless communication range is larger than the highway width such that we consider only the 1-D distance along the highway; i.e., the highway width is neglected. Also, for the medium access control (MAC) layer protocol in a VANET, the IEEE 802.11 distributed coordination function (DCF) is assumed. Additionally, the Nakagami-m distribution [21] is used for the radio channel propagation model, [22]. Finally, the constant bit rate (CBR) pattern is considered for the packet traffic model between the source and destination.

IV. CDF FOR THE END-TO-END DELAY

As mentioned in the system model, the inter-vehicle packet transmission within the communication range is assumed to be instantaneous. Therefore, it is assumed that the only delay in packet propagation occurs when the packet is being carried by a vehicle in the carry-and-forward strategy (re-healing delay). In addition, a VANET may have many gaps over a stretch of highway. Consequently, the end-to-end delay is equal to the sum of the re-healing delays between the source and the destination.

Firstly, from [15], the closed-form expression for the unconditional single re-healing delay is shown in Eq. (1). On the other hand, from [18], the PMF for the number of gaps conditioned on distance is as follows

$$Pr[N_{gaps} = m | D = a] = e^{-\lambda a}\sum_{i=m}^{\lfloor a/r\rfloor}\frac{(-1)^{i-m}}{m!(i-m)!}\left[-\lambda(a-ir)\right]^{i-1}$$
$$\left(i+\lambda(a-ir)\right)e^{-\lambda(a-ir)}, \quad (2)$$

where r is the vehicle wireless communication range, and a is the distance between source and destination. The maximum number of gaps in this distance is $\lfloor a/r\rfloor$.

Therefore, we can obtain the PDF of the end-to-end delay conditioned on the distance between source and destination. $Pr[T_d = t | D = a]$

$$= \sum_{i=0}^{\lfloor a/r\rfloor}\left[f_{T_r}(t) *^i f_{T_r}(t)\right] Pr[N_{gaps} = i+1 | D = a], \quad (3)$$

where $*^i$ represents the convolution iterated i times between the unconditional PDF for the re-healing delay and itself. We derived the closed form for the unconditional PDF for the

re-healing delay by differentiating $F_{T_r}(t)$. The closed form expression for the unconditional PDF of the re-healing delay is

$$f_{T_r}(t) = \frac{-2\Delta v\,(\lambda t+1)}{t^2\lambda\,(-2v_{\min}+\Delta v)^2}\Big(\Delta v k_1\lambda t - 2k_1 v_{\min}\lambda t + \Delta v k_1 - \Delta v k_2 + 2k_1 v_{\min} - 2k_2 v_{\min}\Big)$$

where

$$k_1 = e^{\frac{-2\lambda(t\Delta v+r)}{2v_{\min}+\Delta v}},\ k_2 = e^{-\frac{\lambda\left(t\Delta v+2tv_{\min}+2r\right)}{2v_{\min}+\Delta v}}. \tag{4}$$

Moreover, the CDF of the end-to-end delay conditioned on the distance is

$$Pr[T_d<t|D=a] = \int_0^t \sum_{i=0}^{\lfloor a/r\rfloor} [f_{T_r}(t_r)\ *^i\ f_{T_r}(t_r)]\ Pr[N_{gaps}=i+1|D=a]\ dt_r, \tag{5}$$

where the ith term in the summation represents the sum of the delays conditioned on having i gaps in that distance a.

Next, we can switch the order of integration and summation to obtain

$$Pr[T_d<t|D=a] = \sum_{i=0}^{\lfloor a/r\rfloor} [F_{T_r}(t)\ *^i\ f_{T_r}(t_r)]\ Pr[N_{gaps}=i+1|D=a]. \tag{6}$$

In addition, we can change the $*^i$ to multiplication by taking the Fourier transform of $f_{T_r}(t)$ as shown in Eq. (7). One can obtain closed forms for the Fourier transforms of $f_{T_r}(t)$ and $F_{T_r}(t)$. However, it is a challenge to get the inverse Fourier transform of the entire sum shown in Eq. (7).

$$\begin{aligned} Pr[T_d<t|D=a] &= \sum_{i=0}^{\lfloor a/r\rfloor} \mathscr{F}_t^{-1}\Big[[f_{T_r}(\omega)]^i\,F_{T_r}(\omega)\Big]\ Pr[N_{gaps}=i+1|D=a] \\ &= \mathscr{F}_t^{-1}\left[\sum_{i=0}^{\lfloor a/r\rfloor} [f_{T_r}(\omega)]^i\,F_{T_r}(\omega)]\ Pr[N_{gaps}=i+1|D=a]\right], \end{aligned} \tag{7}$$

where, $f_{T_r}(\omega)$ and $F_{T_r}(\omega)$ are the the Fourier transforms of $f_{T_r}(t)$ and $F_{T_r}(t)$, respectively.

V. Lower Bound for the End-to-end Delay PDF

The most challenging part of Eqs. (3) and (6) is the repeated convolution of the unconditional PDF for the re-healing delay. We start by simplifying $F_{T_r}(t)$, the CDF of the unconditional re-healing delay by ignoring some terms. In Eq. (1), one can note that $F_{T_r}(t)$ has three main terms (the first term has in the denominator $t(v_{\max}+v_{\min})\left(\lambda+\frac{2(\lambda v_{\min}-\lambda v_{\max})}{v_{\max}+v_{\min}}\right)^2$, the second one is $e^{-\left(k_2-k_1+\frac{2\lambda r}{v_{\max}+v_{\min}}\right)}$, and the third term is equal to 1). In addition, The general form of $F_t(t_r)$ is as follows,

$$\frac{e^{at}(bt+c)}{mt} - e^{kt} + 1, \tag{8}$$

where a, b, c, m, and k are functions of the other parameters (λ, $v_{\max}$, $v_{\min}$, r). It is difficult to obtain the Laplace or Fourier transform of this expression after raising it to the power i. The most challenging problem results from the first term $\frac{e^{at}(bt+c)}{mt}$. Therefore, we can simplify the CDF of the unconditional re-healing delay by replacing the first term with another term that is lower than the first term $\frac{e^{at}(bt+c)}{mt}$ and is a function in the second term e^{kt}. Consequently, we will have a lower bound for the CDF of the unconditional re-healing delay. We replaced this term by the following expression, $-\frac{v_{\max}+v_{\min}}{v_{\max}-v_{\min}}e^{-(k_2-k_1)}$, giving a good lower bound. In this case, a lower bound for the unconditional re-healing delay is as follows

$$F_{T_r}(t) = \left(-\frac{v_{\max}+v_{\min}}{\Delta v}e^{\left(\frac{2\lambda r}{v_{\max}+v_{\min}}\right)} - 1\right)e^{-\left(k_2-k_1+\frac{2\lambda r}{v_{\max}+v_{\min}}\right)} + 1$$

where

$$k_1 = 2\lambda v_{\min}t/(v_{\max}+v_{\min}),\ k_2 = 2\lambda v_{\max}t/(v_{\max}+v_{\min}). \tag{9}$$

Therefore, the general form for the lower bound now is as follows

$$\begin{aligned} &F_{T_r}(t) = ae^{bt}+1 \\ &\text{where} \\ &a = -\frac{v_{\max}+v_{\min}}{\Delta v} - e^{\left(\frac{-2\lambda r}{v_{\max}+v_{\min}}\right)},\ b = -k_2+k_1. \end{aligned} \tag{10}$$

In addition, a lower bound on the PDF of the unconditional re-healing delay is as follows

$$f_{T_r}(t) = ce^{bt}, \tag{11}$$

where $c=ab$. On the other hand,

$$\mathscr{L}_t[ce^{bt}] = \frac{c}{s-b} \tag{12}$$

and

$$\mathscr{L}_s^{-1}\left[\left(\frac{c}{s-b}\right)^i\right] = \frac{t^{i-1}c^ie^{bt}}{(i-1)!}. \tag{13}$$

Finally, a lower bound on the PDF of the end-to-end delay conditioned on the distance from source to destination is

$$\begin{aligned} Pr[T=t|D=a] = &\sum_{i=1}^{\lfloor a/r\rfloor} \frac{t^{i-1}c^ie^{bt}}{(i-1)!}e^{-\lambda a} \\ &\sum_{k=i+1}^{\lfloor a/r\rfloor} \frac{(-1)^{k-i-1}}{(i+1)!(k-i)!}\,[-\lambda(a-kr)]^{k-1} \\ &(i+1+\lambda(a-kr))\,e^{-\lambda(a-kr)}, \end{aligned} \tag{14}$$

where

$c = \left(\frac{2\lambda t\Delta v}{v_{\max}+v_{\min}}\right)\left(\frac{v_{\max}+v_{\min}}{\Delta v}+e^{\left(\frac{-2\lambda r}{v_{\max}+v_{\min}}\right)}\right)$, and

$b = \frac{-2\lambda t\Delta v}{v_{\max}+v_{\min}}$.

The detailed derivation of the proof for inequalities of this expression is included in the Appendix.

VI. Upper Bound for the End-to-end Delay

Here, we follow the same methodology for calculating the lower bound of the end-to-end delay. For the upper bound, we replace the first term in the unconditional re-healing delay

CDF by the following term

$$\frac{-2\left(-\Delta v+\frac{(2\Delta v)^2}{4v_{\max}+v_{\min}}\right)}{(v_{\max}+v_{\min})\left(1-\frac{2\Delta v}{v_{\max}+v_{\min}}\right)^2}e^{-\left(k_2-k_1+\frac{2\lambda r}{v_{\max}+v_{\min}}\right)}. \quad (15)$$

In this case, an upper bound for the unconditional re-healing delay is as follows

$$F_{T_r}(t)=\left(\frac{-2\left(-\Delta v+\frac{(2\Delta v)^2}{4v_{\max}+v_{\min}}\right)}{(v_{\max}+v_{\min})\left(1-\frac{2\Delta v}{v_{\max}+v_{\min}}\right)^2}-1\right) e^{-\left(k_2-k_1+\frac{2\lambda r}{v_{\max}+v_{\min}}\right)}+1. \quad (16)$$

Therefore, the general form for the lower bound now is as follows

$$F_{T_r}(t)=ae^{bt}+1 \quad (17)$$

where

$$a=\left(\frac{-2\left(-\Delta v+\frac{(2\Delta v)^2}{4v_{\max}+v_{\min}}\right)}{(v_{\max}+v_{\min})\left(1-\frac{2\Delta v}{v_{\max}+v_{\min}}\right)^2}-1\right)e^{-\left(\frac{2\lambda r}{v_{\max}+v_{\min}}\right)},$$

$b=k_1-k_2$.

In addition, an upper bound on the PDF of the unconditional re-healing delay is as follows

$$f_{T_r}(t)=ce^{bt}, \quad (18)$$

where $c=ab$. Then, we follow the same method used before in the lower bound section. Finally, an upper bound on the PDF of the end-to-end delay conditioned on the distance from source to destination is

$$Pr[T=t|D=a]=\sum_{i=1}^{\lfloor a/r\rfloor}\frac{t^{i-1}c^i e^{bt}}{(i-1)!}e^{-\lambda a}$$
$$\sum_{k=i+1}^{\lfloor a/r\rfloor}\frac{(-1)^{k-i-1}}{(i+1)!(k-i)!}\left[-\lambda(a-kr)\right]^{k-1}$$
$$(i+1+\lambda(a-kr))\,e^{-\lambda(a-kr)}$$

where

$$c=\left(\frac{-2\lambda t\Delta v}{v_{\max}+v_{\min}}\right)\left(\frac{-2\left(-\Delta v+\frac{(2\Delta v)^2}{4v_{\max}+v_{\min}}\right)}{(v_{\max}+v_{\min})\left(1-\frac{2\Delta v}{v_{\max}+v_{\min}}\right)^2}-1\right)$$
$$e^{-\left(\frac{2\lambda r}{v_{\max}+v_{\min}}\right)}$$
$$b=\left(\frac{-2\lambda t\Delta v}{v_{\max}+v_{\min}}\right). \quad (19)$$

The detailed derivation of the proof for inequalities of this expression is included in the Appendix.

VII. Simulation and Analysis Validation

This section presents a comparison between the simulation and analytical results. We implemented a routing protocol for the simulation results in NS-2 (V-2.34). In addition, VanetMobiSim [23] is used to generate realistic vehicle mobility scenarios. In this mobility model, a one-way highway segment is considered. The simulation parameters used in these simulations are summarized in Table II.

Table II
Simulation Parameters

Simulation Parameter	Value
Vehicular density λ (veh/s)	0.07, 0.08, 0.09
Highway length (km)	30
Simulation time (s)	500
Minimum speed $v_{\min}$ (m/s)	15
Maximum speed $v_{\max}$ (m/s)	30
Channel date rate (Mbps)	2
Simulation runs	200
Vehicle communication range r (m)	300
a (km)	6

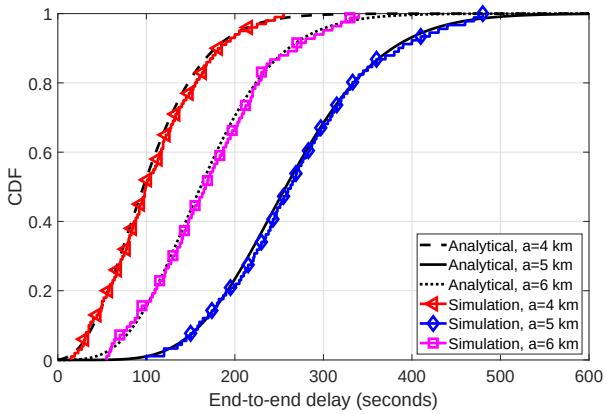

Fig. 2. End-to-end delay while changing a.

A. End-to-end Delay

Fig. 2 shows the proposed analytical results for the end-to-end delay CDF with the same simulation parameters as in Table II and λ=0.08 vehicles/second, while changing the distance between the source and the destination a (4, 5, and 6 km). The analytical results in Fig. 2 are plotted using Eq. (6). One can note that the two curves (analytical, simulation) agree closely across all end-to-end delay values T_d for the three a values, confirming that our model is accurate to characterize the CDF of the end-to-end delay.

However, a small deviation between the simulation and analytical results may be observed. This is because our proposed model assumes that the delay in receiving and processing packets before they are available for further relaying is neglected.

On the other hand, results show that a has a high impact on the CDF of the end-to-end delay. For instance, the CDF of the end-to-end delay at a is equal to 4 km is the highest CDF for all values of end-to-end delay T_d. This is because decreasing a causes a decrease in the end-to-end delay.

In addition, decreasing a increases the probability that there are no gaps between the source and the destination based on

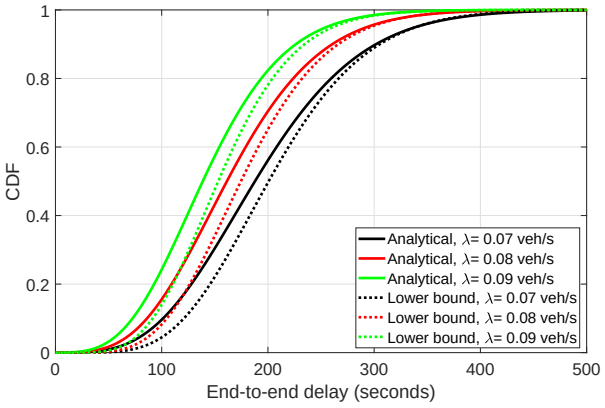

Fig. 3. Results for lower bound expression while changing λ.

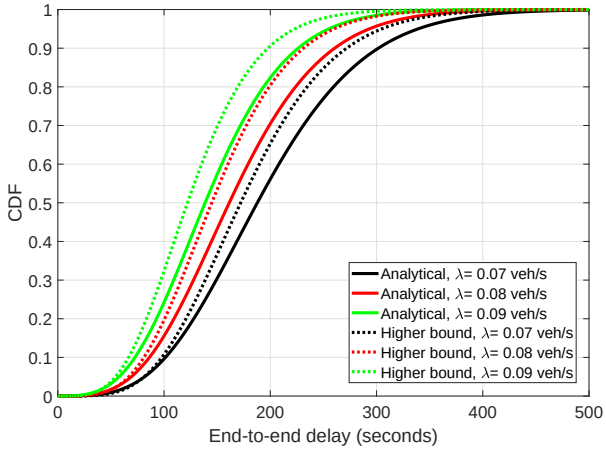

Fig. 4. Results for upper bound expression while chnaging λ.

the PMF of the gaps conditioned on the distance as shown in Eq (2).

B. Lower Bound for CDF on the End-to-End Delay

Fig. 3 shows the analytical CDF and lower bound results for the CDF of the end-to-end delay while changing the vehicular density λ to values of 0.07, 0.08, and 0.09 vehicles/second, and the other parameters as in Table II with a equal to 6 km. The analytical results in Fig. 3 is plotted using Eq. (6). In addition, the lower bound results in Fig. 3 is plotted using Eq. (14).

One can note that there is no large difference between the two curves for the three vehicular densities, indicating that our closed form for the lower bound of the end-to-end delay PDF is good in characterizing the end-to-end delay especially at small and large values of t. However, at middle values of T_d, we can note a slight difference between the lower bound and the analytical results especially at larger values of end-to-end delay T_d.

For instance, at $T_d = 100$, the values of the analytical CDF for vehicular densities 0.07, 0.08 and 0.09 vehicles/second are 0.09, 0.15, and 0.23, respectively. However, the lower bound for the CDF for vehicular densities 0.07, 0.08 and 0.09 vehicles/second are 0.04, 0.07, and 0.13, respectively. On the other hand, at $T_d = 200$ seconds, the values of the analytical CDF for vehicular densities 0.07, 0.08 and 0.09 vehicles/second are 0.55, 0.69, and 0.81, respectively. However, the values of the lower bound of the CDF for vehicular densities 0.025, 0.035 and 0.045 vehicles/second are 0.49, 0.64, and 0.77, respectively.

C. Upper Bound for CDF on the End-to-End Delay

Fig. 3 shows the analytical CDF and lower bound results for the CDF of the end-to-end delay when changing the vehicular density λ to values of 0.07, 0.08, and 0.09 vehicles/second, and the other parameters as in Table II with a equal to 6 km.

Fig. 4 shows the analytical CDF and lower bound results for the CDF of the end-to-end delay with changing the vehicular density λ to values of 0.07, 0.08, and 0.09 vehicles/second, and the other parameters as in Table II. The analytical results in Fig. 4 are plotted based on Eq. (6). In addition, the upper bound results in Fig. 4 are plotted based on Eq. (19).

One can note that there is no large difference between the two curves for the three vehicular densities, indicating that our closed form for the upper bound of the end-to-end delay PDF is good in characterizing the end-to-end delay especially at small values of t . However, at larger values of t, we can note a slight difference between the upper bound and the analytical results.

For instance, at $t = 100$ seconds the values of the analytical CDF for vehicular densities 0.07, 0.08 and 0.09 vehicles/second are 0.09, 0.15, and 0.23, respectively. However, the lower bound for the CDF for vehicular densities 0.025, 0.035 and 0.045 vehicles/second are 0.11, 0.20, and 0.31, respectively. On the other hand, at $t = 200$ seconds, the values of the analytical CDF for vehicular densities 0.07, 0.08 and 0.09 vehicles/second are 0.55, 0.69, and 0.81, respectively. However, the values of the lower bound of the CDF for vehicular densities 0.07, 0.08 and 0.09 vehicles/second are 0.7, 0.81, and 0.9, respectively.

D. Results compared with related work

Fig. 5 presents the analytical results for the proposed model and that proposed in Refs. [4] and [16] for the CDF of the end-to-end delay with a equal to 15 km, r equal to 250 m, and $(v_{\min}, v_{\max})$ equal to (15, 25) m/sec, and changing the vehicular density λ to values 0.07, 0.08, and 0.09 vehicles/second. The analytical results in Fig. 5 are plotted using Eq. (6).

The results confirm that there there is a difference between the proposed result and those from Refs. [4] and [16], especially for low vehicular densities. This is because the analysis in Refs. [4] and [16] is based on the analytical expression of unconditional re-healing delay proposed in Ref. [4] as follows

$$P(T_r < t | L = l) = \int_0^{\infty} f_{X(t)}(x) \int_0^{x+r-l} f_{X'(t)}(x')\, dx'\, dx, \qquad (20)$$

where $l > r$ and l is the gap length between two VANET clusters. However, Refs. [4] and [16] proposed a correction

for this expression as follows

$$P(T_r < t | L = l) = \int_{(l-r)v_{\max}/\Delta v}^{\infty} f_{X(t)}(x)\, F_{X'(t)}(x+r-l)\, dx. \quad (21)$$

This expression is revised because the two clusters are moving simultaneously. Consequently, the minimum re-healing delay required is $(\frac{l-r}{\Delta v})$ seconds (when the head of the first cluster is moving with $v_{\max}$ and the tail of the next cluster is moving with $v_{\min}$). As a result, the minimum distance the cluster head should move before re-healing is $(l-r)v_{\max}/\Delta v$. Therefore, the limits of integration respect to x in Eq. (20) should be between $(l-r)v_{\max}/\Delta v$ x and ∞ as in Eq. (21).

In addition, the difference is decreased at high vehicular densities, as an increase in the vehicular density leads to a decrease in the number of gaps in VANETs based on the PMF of the number of gaps as mentioned in Eq. (2). Therefore, the difference between the proposed expression for the end-to-end delay and Refs. [4] and [16] decreases for high vehicular densities, as the impact of the error in the expression of the re-healing delay does not dominate the CDF of the end-to-end delay values. In the simulation section of Refs. [4] and [16], the authors used vehicular density values which were more than 0.2 vehicles/second. Therefore, the simulations and analytical results were close. On the contrary, for low vehicular densities, the difference between the proposed expression and those from Refs. [4] and [16] is increased. This is because low vehicular densities lead to a greater number of gaps. Consequently, the error in Eq. (20) has a larger impact on the CDF of the end-to-end delay.

Furthermore, the proposed analytical expression for the end-to-end delay probability distribution has a lower-complexity as it is based on PMF of the number of gaps from source to destination, and the closed-form expression for the probability density distribution of a single re-healing delay (this paper model has one summation over iterated convolutions over the closed-form expression for the PDF of the re-healing delay, while Ref. [16] is based on a summation over repeated convolutions of a numerically-calculated double integral). While Ref[4] is based on analytical expression for the CDFs of the distances travelled by the head and tail of a cluster, Ref. [16] is based on closed-form expressions for both CDFs. Therefore, the expression in Ref. [4] has higher complexity than the one from Ref. [16].

Finally, there is a small difference between the results of Refs. [4] and [16]. In [16], closed-form expressions for the CDFs of the distances travelled by the head and tail of a cluster were used, while Ref. [4] used analytical expressions for both CDFs which involved unsimplified integrals.

On the other hand, we can note that the vehicular density λ has a high impact on the CDF of the end-to-end delay. This is because increasing the vehicular densities decreases the re-healing delay due to decreased gap length. At the same time, based on the PMF for the number of gaps as mentioned in Eq (2), the number of gaps (re-healing delays) between source and destination decreased with increasing vehicular densities.

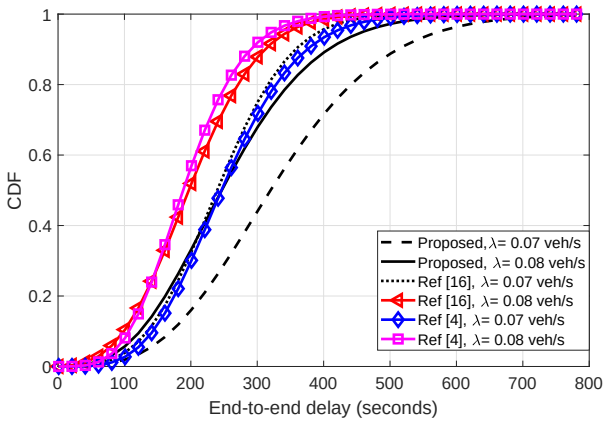

Fig. 5. Results for the proposed compared with the previous work.

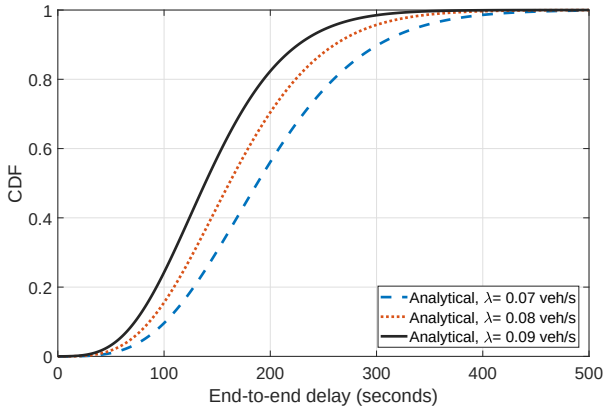

Fig. 6. End-to-end delay with changing λ.

VIII. Impact of other parameters of VANETs

Here, we show the impact of VANET parameters (vehicular density λ, vehicle wireless communication range r, varying speed range Δv with the same average speed, and varying average speeds with the same Δv) on the CDF of the end-to-end delay. It was found through simulation that the accuracy was similar to those in the previous section. Therefore, only the analytical plots are shown below for clarity.

A. Vehicular density

Fig. 6 presents the analytical results for the CDF of the end-to-end propagation delay while changing the vehicular density to values 0.07, 0.08, and 0.09 vehicles/second with a equal to 6 km, and the same parameters of simulation as in Table II. The analytical results in Fig. 6 are plotted using Eq. (6).

It can be seen that the vehicular density λ has a high impact on the CDF of the end-to-end delay. This is because increasing the vehicular density decreases the re-healing delay due to decreased gap length. At the same time, increasing the vehicular density decreases the number of gaps in VANETs based on the PMF of the number of gaps as mentioned in Eq. (2).

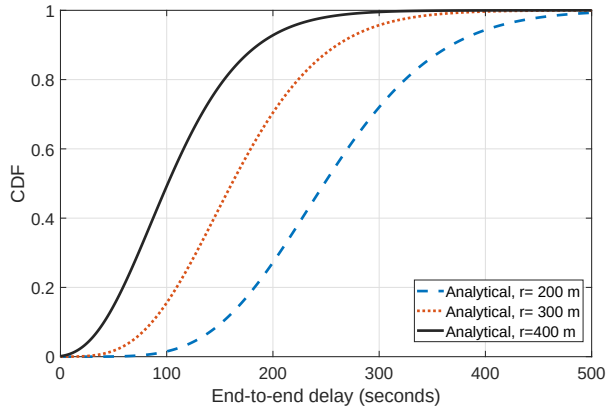

Fig. 7. End-to-end delay with changing r.

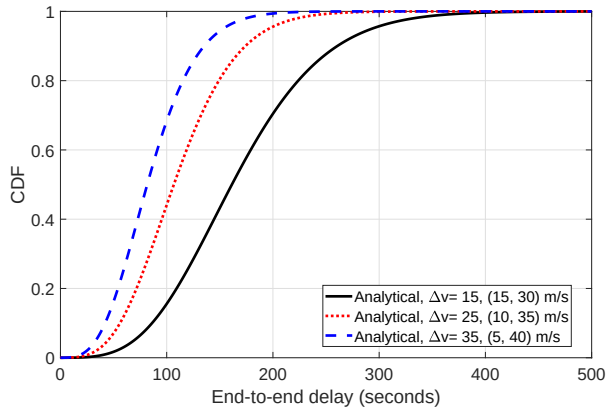

Fig. 8. End-to-end delay with changing the minimum and maximum speeds.

B. Wireless communication range

Fig. 7 presents the analytical results for the CDF of the end-to-end delay with the simulation parameters in Table II and λ=0.055 vehicles/second, and a equal to 6 km, while changing the vehicle wireless communication range r (200, 300, and 400 m). The analytical results in Fig. 7 are plotted using Eq. (6).

The results confirms that the value of the radio wireless range r highly impacts the CDF of the end-to-end delay. As an example, at r equal to 400 m, the CDF of the end-to-end delay is the highest for all values of T_d. This is because increasing r causes a decrease in the re-healing delay. In addition, increasing r decreases the re-healing distances between the clusters as well as the number of clusters in the VANET based on the PMF in Eq (2).

In addition, especially in high vehicular densities, this difference increases. Therefore, we plot it at higher vehicular densities (λ=0.8 vehicles/sec). This is because, at low vehicular densities, the packet will have excessive carry-and-forward stages because the number of gaps increases. At the same time, r does not have a large effect on the re-healing delay in the case of a carry-and-forward strategy.

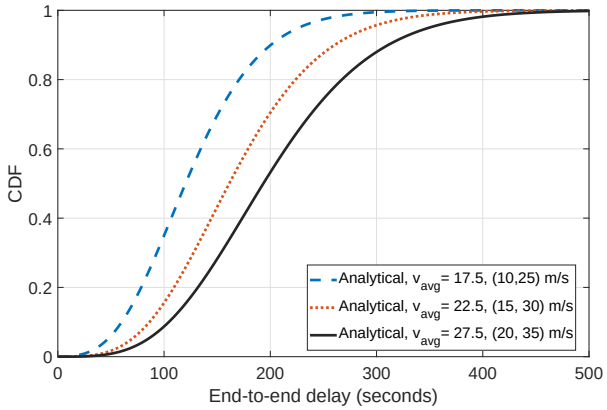

Fig. 9. End-to-end delay with changing average speed.

C. Speed range

Fig. 8 presents the analytical results for the CDF of the end-to-end delay with the parameters of simulation in Table II, λ=0.025 vehicles/second, and a set to 6 km, while changing the speed range Δv ((15,30), (10,35), (5,40) m/s) and keeping the same value for the average speed 22.5 m/s. The analytical results in Fig. 8 are plotted using Eq. (6).

Results confirms that the speed range impacts the CDF of the end-to-end delay. As an example, the CDF of the end-to-end delay at speed range equal to 35 m/s is the highest CDF for the all values of T_d. This is because increasing the speed range leads to an increase in the relative speed between every two successive clusters. As a result, the re-healing delay decreases. Consequently, the CDF of the end-to-end delay increases. This is because the speeds have an impact on the the CDF of single re-healing delay. Consequently, the end-to-end delay changes.

D. Average Speed

Fig. 9 presents the CDF of the end-to-end delay results with the parameters of simulation in Table II, λ=0.08 vehicles/second, and a set to 5 km, while changing the average speed (17.5, 22.5, and 27.5 m/s), and keeping the same value for the speed range Δv = 15 m/s. The analytical results in Fig. 9 are plotted using Eq. (6).

Results show that the average speed impacts the CDF of the end-to-end delay. As an example, the CDF of the end-to-end delay for average speed 17.5 m/s is the highest in case of all values of T_d. This is expected as in the summation, the values of $v_{\min}$ and $v_{\max}$ have an impact on the single re-healing delay. Based on Eqs. (4) and (9) for the CDF and PDF the re-healing delay, respectively, there are many terms that have the sum of $v_{\min}$ and $v_{\max}$ in the denominator. Therefore, increasing the sum of $v_{\min}$ and $v_{\max}$, leads to a decrease in the values for PDF and CDF of of the re-healing delay. Consequently, the CDF of the end-to-end delay decreases as it depends on the re-healing delay and the number of gaps in the routing path. In our plot, the sum of $v_{\min}$ and $v_{\max}$ in the case of average speed 27.5 m/s is the highest. Therefore, the CDF of the end-to-end delay for average speed 27.5 m/s is the lowest in case of all values of T_d.

IX. General Discussion

In this section, we give comments and general discussion related to results from the previous section.

We find that the CDF of the end-to-end packet delivery delay is based on a convolution between the CDF of a single re-healing delay and the PMF of the number of gaps. Therefore, any parameter that has an impact on both the CDF of a single re-healing delay and the PMF of the number of gaps, will be expected to have the most significant effect on the CDF of the end-to-end delay. Therefore,

1) The vehicular density λ has the most significant impact on the CDF of the unconditional re-healing delay. Increasing λ causes an increase in the CDF of the end-to-end delay. This is because increasing the vehicular density decreases the re-healing delay due to shorter gap lengths. At the same time, increasing the vehicular density decreases the number of gaps in the routing path based on the PMF for the number of gaps in Eq. (2).
2) The distance between the source and the destination a has the second most significant impact on the CDF of the end-to-end delay. This is because a has an significant impact on the PMF of the number of gaps. With increasing a also increases, the number of gaps in the distance a. Consequently, there is an increase in the upper limit of the summation in Eq. (6).
3) The wireless communication range r has the third most significant impact on the CDF of the end-to-end propagation delay. Increasing r leads to an increase in the CDF of the end-to-end propagation delay. This is because r has an effect on both the CDF of a single re-healing delay and the PMF of the number of gaps.
4) Finally, the speed parameters ($v_{\min}$, $v_{\max}$, Δv) have the fourth most significant impact on the CDF of the end-to-end delay. This is because the speeds have an impact only on the CDF of the unconditional re-healing delay.

X. CONCLUSION

In this paper, we obtained an analytical formula for the end-to-end delay probability distribution based on the PMF of the number of gaps from source to destination and the closed form expression of the re-healing delay in one way VANET. Furthermore, a closed-form expression for the lower bound of the end-to-end delay probability density distribution was obtained, allowing a service provider to rapidly find a bound on the worst-case end-to-end delay for a VANET. In addition, we derived a closed-form expression for the upper bound of the probability distribution of the end-to-end delay conditioned on the distance between the source and the destination in a VANET. Extensive computer simulation results demonstrated the accuracy of our analysis. Simulation results verified the accuracy of our analytical model and reflected the relation between the end-to-end delay and the VANET parameters such as wireless communication range, vehicular density, the distance between the source and the destination, and minimum and maximum vehicle speed on the end-to-end delay. We will consider a two-way highway in future work.

Appendix

A. Lower Bound for the End-to-end Delay PDF

We can assume the first term in Eq. (1) with denominator $t(v_{\max}+v_{\min})\left(\lambda+\frac{2(\lambda v_{\min}-\lambda v_{\max})}{v_{\max}+v_{\min}}\right)^2$, is equal to

$$e^{-\left(k_2+k_1+\lambda t+\frac{2\lambda(r-v_{\min}t)}{v_{\max}+v_{\min}}\right)}(A). \tag{22}$$

Now, we wish to prove that

$$e^{-\left(k_2+k_1+\lambda t+\frac{2\lambda(r-v_{\min}t)}{v_{\max}+v_{\min}}\right)}(A) > -\frac{v_{\max}+v_{\min}}{\Delta v}e^{-(k_2-k_1)}, \tag{23}$$

After simplification, this is equivalent to

$$A > -\frac{v_{\max}+v_{\min}}{\Delta v}e^{\left(\lambda t+k_1+\frac{2\lambda r}{v_{\max}+v_{\min}}\right)}, \tag{24}$$

Then, substituting A by its value and multiplying both sides by -1

$$\begin{aligned}&\frac{(\Delta v)^2\lambda\left(e^{k_2}+e^{k_1+\lambda t}\left(\lambda t-1-\frac{2\lambda t\Delta v}{v_{\max}+v_{\min}}\right)\right)}{\lambda^2 t(v_{\max}+v_{\min})^2\left(1-\frac{2\Delta v}{v_{\max}+v_{\min}}\right)^2}\\&< e^{\lambda t+k_1+\frac{2\lambda r}{v_{\max}+v_{\min}}},\end{aligned} \tag{25}$$

Then, dividing both sides by $e^{\lambda t+k_1}$

$$\begin{aligned}&\frac{(\Delta v)^2\left(e^{k_2-k_1-\lambda t}+\left(\lambda t-1-\frac{2\lambda t\Delta v}{v_{\max}+v_{\min}}\right)\right)}{\lambda t(v_{\max}+v_{\min})^2\left(1-\frac{2\Delta v}{v_{\max}+v_{\min}}\right)^2}\\&< e^{\frac{2\lambda r}{v_{\max}+v_{\min}}},\end{aligned} \tag{26}$$

This can be expressed in the equivalent form

$$\begin{aligned}&(\Delta v)^2\left(e^{k_2-k_1-\lambda t}+\lambda t-1-\frac{2\lambda t\Delta v}{v_{\max}+v_{\min}}\right)<\\&\lambda t e^{\frac{2\lambda r}{v_{\max}+v_{\min}}}(v_{\max}+v_{\min})^2\left(1-\frac{2\Delta v}{v_{\max}+v_{\min}}\right)^2,\end{aligned} \tag{27}$$

However, we have $1+x\le e^x$, so we can replace $e^{k_2-k_1-\lambda t}$ by $1+k_2+-k_1-\lambda t$ as follows

$$\begin{aligned}&(\Delta v)^2\left(k_2-k_1-\frac{2\lambda t\Delta v}{v_{\max}+v_{\min}}\right)<\\&\lambda t(v_{\max}+v_{\min})^2\left(1-\frac{2\Delta v}{v_{\max}+v_{\min}}\right)^2 e^{\frac{2\lambda r}{v_{\max}+v_{\min}}},\end{aligned} \tag{28}$$

In addition, the term $\left(k_2-k_1-\frac{2\lambda t\Delta v}{v_{\max}+v_{\min}}\right)=0$. Consequently, inequality Eq. (23) will be true if and only if

$$\lambda > 0, \tag{29}$$

From the system model, λ is always greater than zero. Therefore, because all the inequalities are equivalent to each other, Eq. (23) is always true.

B. Upper Bound for the End-to-end Delay PDF

Here, we wish to prove that

$$e^{-\left(k_2+k_1+\lambda t+\frac{2\lambda(r-v_{\min}t)}{v_{\max}+v_{\min}}\right)}(A) < \left(\frac{-2\left(-\Delta v+\frac{(2\Delta v)^2}{4v_{\max}+v_{\min}}\right)}{(v_{\max}+v_{\min})\left(1-\frac{2\Delta v}{v_{\max}+v_{\min}}\right)^2}\right)e^{-\left(k_2-k_1+\frac{2\lambda r}{v_{\max}+v_{\min}}\right)}. \quad (30)$$

After substitution of A and multiplication of both terms by

$$\frac{(v_{\max}+v_{\min})\left(1-\frac{2\Delta v}{v_{\max}+v_{\min}}\right)^2 e^{\left(k_2+\lambda t+\frac{2\lambda r}{v_{\max}+v_{\min}}\right)}}{2}, \quad (31)$$

Eq. (30) can be expressed as follows

$$\frac{\Delta v\left(-e^{k_2}-e^{k_1+\lambda t}\left(\lambda t-1-\frac{2\lambda t\Delta v}{v_{\max}+v_{\min}}\right)\right)}{\lambda t} < \left(\Delta v-\frac{(2\Delta v)^2}{4v_{\max}+v_{\min}}\right)e^{\lambda t+k_1}, \quad (32)$$

Then, dividing both terms by Δv

$$\left(-e^{k_2}-e^{k_1+\lambda t}\left(\lambda t-1-\frac{2\lambda t\Delta v}{v_{\max}+v_{\min}}\right)\right) < \lambda t\left(1-\frac{4\Delta v}{4v_{\max}+v_{\min}}\right)e^{\lambda t+k_1}, \quad (33)$$

Then, dividing both terms by $e^{\lambda t+k_1}$

$$-e^{k_2-k_1-\lambda t}-\lambda t+1+\frac{2\lambda t\Delta v}{v_{\max}+v_{\min}} < \lambda t\left(1-\frac{4\Delta v}{4v_{\max}+v_{\min}}\right), \quad (34)$$

In addition, the term $\frac{4\Delta v}{4v_{\max}+v_{\min}}$ is always less than 1. Therefore, the term

$$\left(1-\frac{4\Delta v}{4v_{\max}+v_{\min}}\right), \quad (35)$$

is always positive. Dividing both sides by this term, Eq. (34) simplifies to

$$\frac{\left(-e^{k_2-k_1-\lambda t}-\lambda t+1+\frac{2\lambda t\Delta v}{v_{\max}+v_{\min}}\right)}{t\left(-1+\frac{4\Delta v}{4v_{\max}+v_{\min}}\right)} < \lambda, \quad (36)$$

Finally, because $e^{k_2-k_1-\lambda t} > 1+k_2-k_1-\lambda t$, and substituting k_1 and k_2 by their values, Eq. (30) will be true if and only if

$$0 < \lambda, \quad (37)$$

From the system model, λ is always greater than zero. Therefore, Eq. (30) is always true.

REFERENCES

[1] C. Kaplan, "Gps, cellular, fm speed and safety control devise," Dec. 26 2006, uS Patent App. 11/645,551.

[2] C. Campolo and A. Molinaro, "Multichannel communications in vehicular ad hoc networks: a survey," *IEEE Communications Magazine*, vol. 51, no. 5, pp. 158–169, 2013.

[3] P. K. Sahu, E. H.-K. Wu, J. Sahoo, and M. Gerla, "Bahg: back-bone-assisted hop greedy routing for vanet's city environments," *IEEE Trans. Intell. Transp. Syst*, vol. 14, no. 1, pp. 199–213, 2013.

[4] H. Wu, R. M. Fujimoto, G. F. Riley, and M. Hunter, "Spatial propagation of information in vehicular networks," *IEEE Trans. Veh. Technol*, vol. 58, no. 1, pp. 420–431, 2009.

[5] Z. Zhang, G. Mao, and B. D. Anderson, "On the information propagation process in mobile vehicular ad hoc networks," *IEEE Trans. Veh. Technol*, vol. 60, no. 5, pp. 2314–2325, 2011.

[6] ——, "On the information propagation process in multi-lane vehicular ad-hoc networks," in *Proc. IEEE ICC*, 2012, pp. 708–712.

[7] N. Wisitpongphan, F. Bai, P. Mudalige, V. Sadekar, and O. Tonguz, "Routing in sparse vehicular ad hoc wireless networks," *IEEE J. Sel. Areas Commun*, vol. 25, no. 8, pp. 1538–1556, 2007.

[8] J. Jeong, S. Guo, Y. Gu, T. He, and D. H. Du, "Trajectory-based data forwarding for light-traffic vehicular ad hoc networks," *IEEE Trans. Parallel Distrib*, vol. 22, no. 5, pp. 743–757, 2011.

[9] C. Guo, D. Li, G. Zhang, and Z. Cui, "Data delivery delay reduction for vanets on bi-directional roadway," *IEEE Access*, vol. 4, pp. 8514–8524, 2016.

[10] J. He, L. Cai, P. Cheng, and J. Pan, "Delay minimization for data dissemination in large-scale vanets with buses and taxis," *IEEE Trans. Mobile Comput*, vol. 15, no. 8, pp. 1939–1950, 2016.

[11] J. He, L. Cai, J. Pan, and P. Cheng, "Delay analysis and routing for two-dimensional vanets using carry-and-forward mechanism," *IEEE Trans. Mobile Comput*, vol. 16, no. 7, pp. 1830–1841, 2017.

[12] A. Abdrabou and W. Zhuang, "Probabilistic delay control and road side unit placement for vehicular ad hoc networks with disrupted connectivity," *IEEE J. Sel. Areas Commun*, vol. 29, no. 1, pp. 129–139, 2011.

[13] A. Abdrabou, B. Liang, and W. Zhuang, "Delay analysis for sparse vehicular sensor networks with reliability considerations," *IEEE Trans. Wirel. Commun*, vol. 12, no. 9, pp. 4402–4413, 2013.

[14] J. Yoo, S. Choi, and C.-k. Kim, "The capacity of epidemic routing in vehicular networks," *IEEE Commun. Lett*, vol. 13, no. 6, 2009.

[15] H. Seliem, R. Shahidi, M. H. Ahmed, and M. S. Shehata, "Probability distribution of the re-healing delay in a one-way highway vanet," *IEEE Commun. Lett*, vol. 22, no. 10, pp. 2056–2059, Oct 2018.

[16] R. Shahidi and M. H. Ahmed, "Probability distribution of end-to-end delay in a highway vanet," *IEEE Commun. Lett*, vol. 18, no. 3, pp. 443–446, 2014.

[17] ——, "On the analytical calculation of the probability distribution of end-to-end delay in a two-way highway vanet," *IEEE Access*, 2017.

[18] S.-I. Sou and Y. Lee, "End-to-end performance for scf-based vehicular routing over multiple communication gaps," *IEEE Commun. Lett*, vol. 18, no. 6, pp. 1015–1018, 2014.

[19] K. A. Hafeez, L. Zhao, B. Ma, and J. W. Mark, "Performance analysis and enhancement of the dsrc for vanet's safety applications," *IEEE Trans. Veh. Technol*, vol. 62, no. 7, pp. 3069–3083, 2013.

[20] C. Campolo, A. Molinaro, A. Vinel, and Y. Zhang, "Modeling prioritized broadcasting in multichannel vehicular networks," *IEEE Trans. Veh. Technol*, vol. 61, no. 2, pp. 687–701, 2012.

[21] M. Killat and H. Hartenstein, "An empirical model for probability of packet reception in vehicular ad hoc networks," *EURASIP J. Wirel. Commun. Netw.*, vol. 2009, pp. 4:1–4:12, 2009.

[22] K. Chen, X. Cao, D. Sung *et al.*, "A street-centric routing protocol based on micro topology in vehicular ad hoc networks," *IEEE Trans. Veh. Technol*, vol. PP, no. 99, pp. 1–1, 2015.

[23] J. Härri, F. Filali, C. Bonnet, and M. Fiore, "Vanetmobisim: generating realistic mobility patterns for vanets," in *Proc. ACM VANET 06*, 2006, pp. 96–97.

Hafez Seliem received the B.Sc. and M.Sc. degrees in computer science from Ainshams University, Cairo, Egypt, in 2009 and 2014, respectively. He is currently working toward the Ph.D. degree with Faculty of Engineering and Applied Science at Memorial University of Newfoundland, St John's, Newfoundland and Labrador, Canada. His research interests include vehicular ad-hoc networks, wireless multihop networks, IOT, Big Data, and software design.

REZA SHAHIDI received the M.Eng. and Ph.D. degrees in computer engineering with a specialization in image processing from the Memorial University of Newfoundland in 2003 and 2008, respectively. He was a Post-Doctoral Fellow with The University of British Columbia from 2008 to 2009, where he conducted research on seismic imaging, after which he spent several years working in industry in radar signal and image processing. Since 2015, he has been a Research Associate with the Memorial University of Newfoundland. His research interests include vehicular networks, digital signal and image processing, and ocean remote sensing.

MOHAMED HOSSAM AHMED. received the Ph.D. degree in electrical engineering from Carleton University, Ottawa, in 2001, where he was a Senior Research Associate from 2001 to 2003. In 2003, he joined the Faculty of Engineering and Applied Science, Memorial University of Newfoundland, where he is currently a Full Professor. He is a registered Professional Engineer in the province of Newfoundland, Canada. He has authored over 140 papers in international journals and conferences. His research interests include radio resource management in wireless networks, multi-hop relaying, cooperative communication, vehicular ad-hoc networks, cognitive radio networks, and wireless sensor networks. He received the Ontario Graduate Scholarship for Science and Technology in 1997, the Ontario Graduate Scholarship in 1998, 1999, and 2000, and the Communication and Information Technology Ontario Graduate Award in 2000. His research was supported by NSERC, CFI, QNRF, Bell/Aliant, and other governmental and industrial agencies. He served as the Co-Chair for the Signal Processing Track in ISSPIT'14 and the Co-Chair of the Transmission Technologies Track in VTC'10-Fall, and the multimedia and signal processing symposium in CCECE'09. He serves as an Editor for the IEEE COMMUNICATION SURVEYS AND TUTORIALS and an Associate Editor for the Wiley International Journal of Communication Systems and the Wiley Communication and Mobile Computing. He served as a Guest Editor for a special issue on Fairness of Radio Resource Allocation, the EURASIP JWCN in 2009, and a Guest Editor for a special issue on Radio Resource Management in Wireless Internet and the Wiley Wireless and Mobile Computing Journal in 2003.

Mohamed Shehata Following a B.Sc. degree with honors in 1996 and a M.Sc. degree in computer engineering in 2001 from Zagazig University, Egypt, he obtained his Ph.D. in software engineering in 2005 from the University of Calgary, Canada. Following his Ph.D., he worked as a Post-doctoral Fellow at the University of Calgary on a joint project between the University of Calgary and the Canadian Government, called Video Automatic Incident Detection. After that, he joined Intelliview Technologies Inc. as a Vice-President of the research and development department. In 2013, after seven years in the industry, he joined Faculty of Engineering and Applied Science at MUN as an Assistant Professor of computer engineering. His research activities include courses in computer vision, image processing, data structures, programming, and software design.